PAPER

Screw dislocation in hcp Ti : DFT dislocation excess energies and metastable core structures

To cite this article: Nathalie Tarrat *et al* 2014 *Modelling Simul. Mater. Sci. Eng.* **22** 055016

View the article online for updates and enhancements.

Related content

- Density functional theory investigations of titanium -surfaces and stacking faults
  Magali Benoit, Nathalie Tarrat and Joseph Morillo

- Magnesium interatomic potential for simulating plasticity and fracture phenomena
  Z Wu, M F Francis and W A Curtin

- Orbital-free density functional theory simulations of dislocations in magnesium
  Ilgyou Shin and Emily A Carter

Recent citations

- Convergence of calculated dislocation core structures in hexagonal close packed titanium
  Max Poschmann *et al*

- Screw dislocation mediated solution strengthening of substitutional -Ti alloys - First principles investigation
  P. Kwasniak and H. Garbacz

- Investigation of the shear response and geometrically necessary dislocation densities in shear localization in high-purity titanium
  Chaoyi Zhu *et al*

Screw dislocation in hcp Ti : DFT dislocation excess energies and metastable core structures

Nathalie Tarrat[1,4,5]**, Magali Benoit**[1,5]**, Daniel Caillard**[1]**, Lisa Ventelon**[2]**, Nicolas Combe**[1,3] **and Joseph Morillo**[1,3]

[1] CEMES-CNRS UPR 8011, 29 rue Jeanne Marvig, 31055 Toulouse Cedex, France
[2] CEA Saclay, Serv Rech Met Phys, F-91191 Gif Sur Yvette, France
[3] Université Paul Sabatier, 118 route de Narbonne, F-31062 Toulouse Cedex 9, France

E-mail: nathalie.tarrat@cemes.fr, magali.benoit@cemes.fr and joseph.morillo@cemes.fr

Abstract

An extensive DFT search of (meta)stable structures of the $\frac{a}{3}\langle 1\,1\,\bar{2}\,0\rangle$ screw dislocation in hcp-Ti is presented. It reveals that the stable core structures are never basal but always prismatic. This prismatic core dissociates into two partial dislocations in the same or neighboring prismatic planes depending on the initial position of the dislocation line, leading to either a symmetric or an asymmetric core. An alternative way of defining the core region from an electronic structure point of view is also proposed. It evidences clearly the symmetric or asymmetric character of the cores. We then introduce an ansatz for a straightforward and fast calculation of the excess energy, per unit length of dislocation, of a screw dislocation applicable to DFT calculations, in the cluster approach. The method is first validated on calculations of a $\frac{a}{3}\langle 1\,1\,\bar{2}\,0\rangle$ screw dislocation in hcp-Ti, performed with an EAM potential from which exact excess energies can be extracted. Then, it is shown that it does work in a DFT calculation, through its application to the same screw dislocation in hcp-Ti with an accuracy of 8.4 meV/Å (1.8% of the excess energy for a cluster of 126 atoms per plane normal to the dislocation line). The comparison of the excess energies of the symmetric and assymmetric cores, calculated with the proposed ansatz, reveals that their energy difference is within the uncertainty

---

[4] Author to whom any correspondence should be addressed.
[5] These authors contributed equally to this work.

of the method, which implies that the potential energy surface is very flat and that there could be many metastable core structures in hcp-Ti.

1. Introduction

The dislocation core structure and mobility play an important role in many phenomena of crystal plasticity in metallic systems [1]. For instance, the core properties control the mobility of dislocations, which accounts for the intrinsic ductility or brittleness of solids. Hexagonal compact metals (about 20) are known to be characterized by a wide variety of plastic behaviour (see [2] and [3] for recent reviews) dominated by the movement of dislocations with the shortest Burgers vector: $\frac{a}{3}\langle 1\,1\,\bar{2}\,0\rangle$. For example, simple metals and most of the transition metals have a basal slip plane, but three of them (Zr, Ti and Hf) and a number of rare-earth metals (Gd, Ru, Tb, Hf, Dy and Er) present a dominant prismatic slip plane [1, 3–5]. *In situ* experiments [6] on the dynamics of dislocations in hcp Ti performed in the nineties have evidenced that the mechanism of strong impurities strengthening (by C, O or N) was not the expected one (edge dislocation pinning), but was the increase of the Peierls friction on $\frac{a}{3}\langle 1\,1\,\bar{2}0\rangle$ screw dislocations, leading to a jerky movement of these dislocations. A model based on a locking-unlocking mechanism, between hypothetically stable sessile and metastable glissile configurations of the dislocation in the prismatic plane, was proposed by the authors to explain these properties. Similar results have been obtained in hcp Zr [2] and more recently in bcc Fe [7, 8].

A good knowledge of the intrinsic characteristics of dislocations (structure, stability, mobility, formation, multiplication) as well as the characteristics of their interactions with other defects such as point defects (vacancies, self-interstitials or impurities), grain boundaries or other dislocations appears then as a prerequisite to a good theoretical description of the plastic behaviour of hexagonal close packed (hcp) metals. Since they are extended defects with a long range displacement field, dislocations are more difficult to model than point defects, surfaces, or other kinds of perturbation to the crystalline lattice. While the linear continuum elasticity theory properly describes the long-range elastic strain of a dislocation for length scales beyond a few lattice spacings, it breaks down near the singularity in the region of the dislocation core. The core is often non-trivial, and requires a very accurate atomistic description, since the very large local strains are difficult to reproduce with semi-empirical potentials [9–12], whereas a long-range elastic field is also present.

In the last decades, there has been a great interest in describing the dislocation core by numerical simulations at the atomic level [4, 5, 9–22]. Due to the increase of computing power and to the development of novel algorithms, it has become possible to investigate dislocation cores with first-principles methods. However, up to now, there exist only very few density functional theory (DFT) determinations of the atomic core structure of the $\frac{1}{3}\langle 1\,1\,\bar{2}\,0\rangle$ screw dislocation in hcp metals (Zr or Ti) [18, 19, 21–23]. In a previous paper [23], we have studied the core geometry of this dislocation within the cluster approach with DFT and we have shown that two (meta)stable core structures (a symmetric core and an asymmetric) can be found depending on the origin of the elastic displacement field applied to generate the dislocation before relaxation. Recently, Ghazisaeidi and Trinkle [21] have studied, within an MEAM (mean embedded atom method) interaction model, the relative stability of these two core structures. They applied a strain to these cores at $T = 0$ K and they have found that

the high-energy assymmetric core always reconstructs into the low-energy symmetric core, whatever the direction of the applied strain. Later on, this same MEAM interaction model has been used by Rao *et al* [24] for a systematic search of metastable structures, the determination of the Peierls stress, and of the kink formation energy using very large simulation cells. They confirmed the previous results and evidenced three more metastable core structures among which, one is dissociated in the basal plane. Even if the accuracy of the MEAM model is questionable [25], these results confirm that the question of the existence of numerous metastable dislocation core structures in hcp-Ti and the consequences on the plastic properties of this metal remain still open.

In the aim to provide some answers to these questions, it is essential to be able to (i) explore the configuration space to find out whether other core structures exist, and most importantly, (ii) determine reliably the excess energies of the different core structures and of the barriers between them. The purpose of this paper is therefore to present an extensive DFT search of meta(stable) screw dislocation core structures and, in order to be able to compare their relative stability, to propose an ansatz allowing a straightforward and fast evaluation of the excess energy of screw dislocations in the cluster approach, applicable to DFT calculations. To test the validity of this ansatz, we needed to perform calculations on very large simulation cells to compare their results to the predictions of the elasticity theory. This cannot be done in the DFT scheme. Thus, even if they are not suitable for the description of the exact core structure of dislocations in Ti [23, 25], we performed this part of the study with the embedded atom method (EAM) potential previously used in [23, 25].

After giving the simulation details in section 2, we present in section 3 a simple and straightforward ansatz for the estimation of the excess dislocation energies with a good accuracy, applicable in a DFT calculation in the cluster approach. Using different initial positions (IPs) for the origin of the elastic displacement field applied to generate the $\frac{a}{3}\langle 1\,1\,\bar{2}\,0\rangle$ screw dislocation, different (meta)stable core structures are found. These structures are presented and analyzed in section 4, together with their dissociation in partial dislocations. Finally, in section 5, the electronic structure of the atoms perturbed by the dislocation for the different metastable cores is analysed.

2. Simulation details

From a theoretical point of view, dislocations, which are extended defects, are difficult to model at the atomic scale. Indeed, dislocations induce a long range elastic field and consequently imply the use of very large system sizes. Therefore, it is convenient to simulate infinite straight line dislocations which enables the use of periodic boundary conditions in the line direction and a subsequent reduction of the simulation cell size. In this work, the system (a cluster) was periodic in the direction parallel to the dislocation line and isolated in the two perpendicular directions. In that case, (i) the system size in the directions perpendicular to the dislocation must be large enough to avoid any interaction between the surface of the cluster and the dislocation core and (ii) a given number of layers of atoms at the boundary of the cluster must be kept fixed at the positions they would have in an infinite crystal. One can use approximate fixed positions given by the linear continuum elasticity theory or use more sophisticated approaches where these positions are dynamically updated giving more accurate boundary positions [26]. Different approaches can then be used to relax the dislocation core [26].

In all the simulations presented in this paper (DFT and EAM), the clusters were of pseudo-hexagonal shape in the direction perpendicular to the dislocation line in order to be as close as possible to a cylindrical shape with the lowest possible surface energy. The *x*, *y* and

z directions were, respectively, the [$\bar{1}$ 1 0 0] and the [0 0 0 1] directions and the dislocation line direction $\frac{a}{3}$[1 1 $\bar{2}$ 0]. The DFT calculations have been carried out on a cluster made of two periodically repeated (1 1 $\bar{2}$ 0) atomic planes, which size was fixed at 252 (2 × 126) atoms for the search of the (meta)stable core configurations and with sizes ranging from 52 (2 × 26) to 252 (2 × 126) atoms for the validation of the ansatz for the excess energy calculation. In the EAM potentials simulations, the cutoff distance of the potential imposes to take 14 atomic (1 1 $\bar{2}$ 0) planes perpendicular to the dislocation line in our simulation box. With this number of atomic planes, the size of the 'hexagon' has been varied from 728 to 14378 atoms, i.e. 52 up to 1027 atoms per plane. The relaxations have been performed with the conjugated gradient method.

2.1. DFT calculations

The DFT calculations have been performed with the SIESTA [27] code in which the Kohn–Sham electronic wave functions are developed on a local basis set. The PBE-GGA gradient approximation [28] has been used for the exchange and correlation functional and the pseudo-potential was a Trouiller–Martins [29] one, with the $3p4s3d$ states as valence states. A polarized double-ζ basis set was employed for the $4s$ electrons and a single-ζ basis set was employed for the $3p$ and $4d$ electrons. A 500 Ry real space grid cutoff and a Methfessel-Paxton smearing of order one with an electronic temperature of 200 meV were used in all calculations. A $1 \times 1 \times 12$ k-point mesh was used for the first Brillouin zone sampling. The convergence criteria was set up so that the maximum atomic force was less than 0.02 eV/Å, which was generally obtained after $\simeq$20–30 atomic relaxation steps.

Note that, in a previous study [25], we have computed bulk properties, elastic constants, stacking faults and γ-surfaces with the same functional, basis sets, pseudopotentials and real space grid cutoff and we concluded that these state-of-the-art DFT-pseudopotential calculations are good enough to reach an acceptable description of dislocations.

2.2. Semi-empirical potential calculations

The semi-empirical potential of the EAM type [30] developed by Zope and Mishin [31] (referred to hereafter as ZM) for the TiAl alloy has been used. They fitted their Ti potential to experimental data (lattice parameters: a, c/a, cohesive energy E_c and the five independent elastic constants C_{ij}) and to the *ab initio* DFT volume–pressure curves of various crystal structures (hcp, face-centred cubic (fcc), body-centred cubic (bcc), simple cubic (sc) and ω). Its cutoff distance is in between the fourth and fifth neighbour shells. In a previous study [25] we have found that this model is not completely satisfactory against the description of both the γ-surfaces and the shear elastic constant: EAM models are not able to give the correct hierarchy between the prismatic and the basal stacking fault excess energies. They usually underestimate all the basal faults and overestimate the prismatic ones, leading to an inversion of the relative stability. However, for a given spreading, they can be used for preliminary tests such as size effects or boundary effects. Note that all the EAM simulations presented in this paper have been also carried out with another EAM potential (which was developed by Hammerschmidt *et al* [32] for the description of grain boundaries) and the results were similar.

In all calculations where periodic conditions were applied in a given direction, the simulation cell dimension in that direction was set to at least five times the interaction cutoff in order to avoid any spurious interaction of an atom with its periodic images.
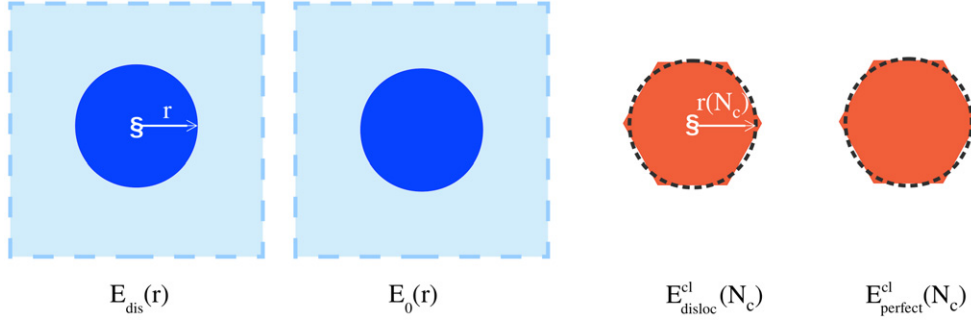
$E_{dis}(r)$ $E_0(r)$ $E^{cl}_{disloc}(N_c)$ $E^{cl}_{perfect}(N_c)$

Figure 1. Schematic representations of, from left to right: Two infinite crystals with and without a dislocation line, where $E_{dis}(r)$ and $E_0(r)$ are the energies stored inside a cylinder of radius r, respectively. Two hexagonal clusters of effective radius $r(N_c)$ (see text) with and without a dislocation line, of respective energies $E^{cl}_{disloc}(N_c)$ and $E^{cl}_{perfect}(N_c)$.

3. Dislocation excess energy

If, as it is the case for the $\frac{a}{3}\langle 1\,1\,\bar{2}\,0\rangle$ screw dislocation in hcp-Ti (see section 4), there exist different stable core structures at $T = 0\,\text{K}$, one needs to know which one is the most stable one and how far they are from each other from an energetic point of view. One thus needs a reliable way to determine their excess energies. In the cluster approach, this can be easily done with a classical interaction model but is not straightforward in DFT as discussed below. In the following, we will show how it is possible to circumvent this problem and get reliable excess dislocation energies, even in DFT calculations in the cluster approach.

The excess energy per unit length of dislocation, stored inside a cylinder of radius r whose axis is the dislocation line in an otherwise infinite crystal is defined as:

$$E_{exc}(r) = E_{dis}(r) - E_0(r), \tag{1}$$

where $E_{dis}(r)$ is the energy of a piece of cylinder of length unity with the dislocation and $E_0(r)$ is the same quantity without the dislocation, i.e. for a perfect crystal (figure 1, left).

In the following, we will define an effective radius $r(N_c)$ associated to a given cluster of N_c atoms and show that, even for small clusters, the defined excess energy (1) is given with a good accuracy by:

$$E^{cl}_{exc}(r(N_c)) = E^{cl}_{exc}(N_c) = (E^{cl}_{disloc}(N_c) - E^{cl}_{perfect}(N_c))/l, \tag{2}$$

where l is the length of the simulation cell in the dislocation line direction, $E^{cl}_{disloc}(N_c)$ is the total energy of the relaxed cluster with the dislocation and $E^{cl}_{perfect}(N_c)$ is the total energy of the corresponding relaxed cluster without the dislocation, provided that both calculations are carried out with the same number of fixed boundary layers (FBLs) at the surface mimicking an infinite crystal (figure 1, right). For the perfect cluster these fixed boundary positions are those of the perfect crystal whereas, for the cluster with the dislocation, we will use approximate positions given by the linear continuum elasticity theory (isotropic or anisotropic).

Our demonstration relies on the verification of the well known linear variation of the excess energy with $\ln(r)$ in the large r limit where the elasticity theory applies [1]:

$$E_{exc}(r) = E_{exc}(r_0) + E_e(r, r_0) = E_{core} + \frac{Kb^2}{4\pi}\ln\left(\frac{r}{r_0}\right), \tag{3}$$
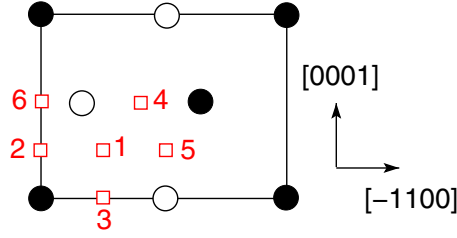
Figure 2. Different IPs of the dislocation line in the unit cell of hcp Ti.

where $E_e(r, r_0)$ is the elastic energy per unit length of the dislocation stored between the cylinders of radius r and r_0, the core radius below which the elasticity theory fails, $E_{exc}(r_0)$ is then the core energy E_{core}. K is a known constant depending on the dislocation type and direction, which expression in the present case is $\sqrt{C_{44}C_{66}}$. Hence, for a given dislocation, this excess energy will be a straight line as a function of $\ln(r)$ for large r values and its slope will not depend on the core structure nor on the precise definition or choice of r_0, nor on the type of calculation, EAM or DFT, as far as they describe properly the elastic constants and the structure of the material under consideration. Consequently, in the following calculations, we did not use the experimentally determined elastic constants but those of the corresponding model, DFT or EAM [25]. Assuming that it is possible to calculate $E_{dis}(r)$ and $E_0(r)$ for different values of r and to define in an unambiguous way r_0, one can extract the values of E_{core} from (3). This is easily done if one uses an approximate description with a classical interaction model where the total energy of the studied cluster reads as a sum of energies per atom over the atoms of the system, and thus it is possible to calculate the energy of a cylindrical piece of crystal centred on the dislocation line for different values of r less than the radius of the cluster. For more sophisticated quantum mechanical calculations within the framework of the DFT, one is faced with the impossibility to apply the preceding method for the two following reasons. First, it is not possible to model systems of such large sizes. Second, one cannot easily define an energy per atom, nor an energy stored in a piece of matter in quantum mechanics since these quantities do not correspond to an observable [33]. Some formulations have nevertheless been proposed [34–38], based on specific expressions of an energy density and the atom-in-molecule approach [39]. However the sole energies which are quantum-mechanically clearly defined are those of a whole cluster containing N_c atoms, i.e. $E_{disloc}^{cl}(N_c)$ and $E_{perfect}^{cl}(N_c)$, and hence $E_{exc}^{cl}(r(N_c))$. Under the hypothesis that a DFT calculation can be performed on a cluster large enough so that the influence of the surface does not extend up to the core region, we will show that it is possible to extract rather accurate values of $E_e(r, r_0)$ and E_{core} from the $r(N_c)$ dependence of $E_{exc}^{cl}(r(N_c))$.

First, using the ZM EAM interaction model for which exact calculations of $E_{exc}(r)$ can be performed we will show that (2) is a good approximation of $E_{exc}(r)$, then we will apply it to DFT calculations. In order to obtain the exact values of $E_{exc}(r)$ versus $\ln r$ a large cluster of 14378 (14×1027) atoms was prepared such that the atoms were positioned following the linear isotropic continuum elasticity theory with an unspread dislocation of Burgers vector $\frac{a}{3}[1\,1\,\bar{2}\,0]$, which centre was set at the IP denoted IP3 in figure 2. Then the atoms of the cluster boundary layer (1 FBL) were kept fixed at the elastic isotropic solution and the other atoms were relaxed using the ZM EAM potential until convergence of the total energy was reached. The final core structure presents a spreading in the prismatic plane (see section 4 and [23] for more details on the core structures).

From this relaxed dislocation structure, we extract the r variation of the excess energy stored in a cylinder of radius r using (1). These $E_{exc}(r)$ values, which are exact excess energies

as far as r is not too close to the radius of the cluster, are plotted as a function of $\ln(r/r_0)$ in figure 3 using black discs, with $r_0 = b$, the Burgers vector. The core radius of a dislocation r_0, originally defined as the distance below which the elasticity theory breaks down [1], is difficult to define unambiguously [1, 10, 40–42]. This is the reason why we have chosen to take it equal to b. Moreover, this core radius value being usually set to b in the literature, this implicit convention allows to make meaningful comparisons between different studies. The results compare very well with the theoretical expression (blue line, equation (3)) even for small r values, reflecting the validity of Peierls–Nabarro type models [1, 40] to describe the energetics of the dislocation to very short distances from the dislocation line.

Let us now turn to our ansatz (2) for the calculation of the excess energy. We first define the radius $r(N_c)$ of an hexagonal cluster of N_c atoms as the radius of the disc leading to the same surface, $\pi r^2(N_c)$, normal to the dislocation line direction as the hexagonal surface, $N_{at}S$, where $N_{at} = N_c/p$ is the number of atoms per surface plane, p the number of planes of the simulation cell and S the surface of the elementary surface cell:

$$r(N_c) = \sqrt{\frac{S}{\pi}} \times N_{at}^{1/2} = \sqrt{\frac{S}{\pi p}} \times N_c^{1/2} = A \times N_c^{1/2} \tag{4}$$

with $p = 14$ and hence $A = 0.522$ Å in the ZM EAM calculation. For different cluster sizes, ranging from $N_c = 14 \times 26$ to 14×610 atoms, excess energies $E_{exc}^{cl}(N_c)$ have been computed as defined in (2) with the same boundary conditions (1 isotropic FBL) and initial position IP3. All core structures relax in the same final prismatic symmetric core (see section 4). The resulting excess energies $E_{exc}^{cl}(r(N_c)) = E_{exc}^{cl}(N_c)$ are then plotted as a function of $r(N_c)$ given by (4) (blue squares in figure 3). These excess energies values obtained using clusters of different sizes with 1 isotropic FBL coincide almost exactly with the exact excess energies (black discs) even for very small clusters, validating our ansatz for the calculation of the excess energy. For large clusters the error is totally negligible and for the smallest considered cluster (26 atoms per plane, 9.95 Å radius), the error is less than $\approx$6 meV/Å, i.e. 1.5% of the excess energy.

The accuracy of our approximation of the excess energy calculation can be easily explained. The error made in this approximation has three distinct origins: the presence of the surface, the hexagonal shape of the cluster and the use of approximate boundary conditions.

The use of the same approximate boundary conditions, in the calculation of $E_{disloc}^{cl}(N_c)$ and $E_{perfect}^{cl}(N_c)$ leads to an efficient elimination of the surface effect in their difference, i.e. the excess energy. This cancellation of the surface is particularly efficient in the case of a screw dislocation, since the dislocation and the surface displacement fields are essentially orthogonal and their displacement fields have their largest values in different regions of the cluster, leading to a very small interaction energy between the two displacement fields and thus an almost complete removal of the surface contribution.

The error due to the non cylindrical shape of the cluster is confined at the surface and thus can be described in terms of elastic energy. There is then an efficient compensation between the missing and the extra atoms of the cluster around $r(N_c)$, compared to the extracted cylinder from the bulk, since they are in equal number and their energies are not much different due to the $\ln r$ elastic dependence of the excess energy.

Thus we obtain a very efficient cancellation of the errors introduced in our calculations for large $r(N_c)$ values. However, as $r(N_c)$ decreases, the cancellation is less and less efficient leading to the observed small increasing deviation at low $r(N_c)$ values.

Next, it is interesting to investigate how the accuracy of the excess energies given by our ansatz (2) depends on the type of approximate boundary conditions. A panel of different approximate boundary conditions have been applied: 1 FBL at the anisotropic elasticity positions, 2 and 3 FBL at the isotropic elasticity positions. Using the anisotropic elasticity
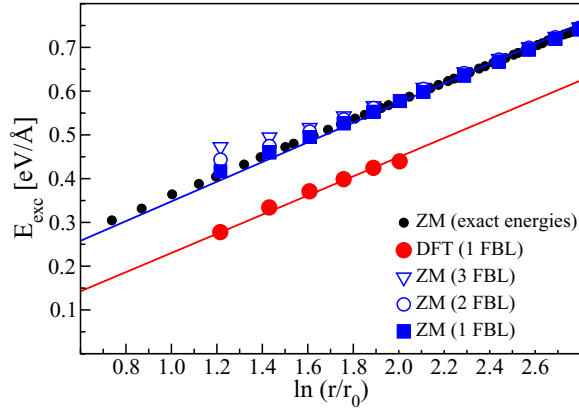
Figure 3. Excess energies in eV/Å as a function of $\ln(r/r_0)$, where $r_0 = b$ is the Burgers vector, for dislocations with a prismatic spreading. Black discs: excess energies (equation (1)) stored within a cylinder of radius r centred at the dislocation line in a 143 78 (14 × 1027) atoms cluster, computed with the ZM EAM potential with 1 FBL at the isotropic elasticity theory positions and initial position IP3 leading to a symmetric prismatic core. Blue symbols: excess energies deduced from cluster ZM EAM calculations (equations (2) and (4)), with 1 (squares), 2 (empty circles) or 3 (empty triangles) FBL at the isotropic elasticity theory positions. Red discs: excess energies deduced from cluster DFT calculations (equations (2) and (4)), with 1 FBL at the isotropic elasticity theory positions and initial position IP1 leading to an asymmetric core. The red and blue lines correspond to (3) with appropriate core energies to best fit respectively the red discs and the blue squares.

instead of the isotropic one with also 1 FBL, a very similar accuracy was obtained, leading to indistinguishable points in figure 3 (and thus not reported on the figure), the largest difference concerns the smallest cluster and is within the accuracy of the calculation (≈ 1 meV/Å). The blue empty circles and triangles in figure 3 show the excess energies obtained for 2 and 3 FBLs at the isotropic elasticity positions, respectively. One can observe that the excess energies are very similar for large clusters whatever the number of FBLs. However there is an increasing deviation from the straight line with the number of FBLs at the isotropic elasticity positions for small cluster sizes. This result evidences that, what is critical to obtain a good accuracy with (2), is not the type of approximate boundary conditions (isotropic or anisotropic from elasticity theory) but the number of fixed layers which must be fixed at one. The reason is that, when a larger number of boundary layers are constrained to approximate boundary conditions, the obtained dislocation has a structure which is more and more different from its exact relaxed structure close to the surface whereas, at the same time, the structure of the perfect cluster is closer and closer to the perfect crystal structure, an effect which increases with decreasing cluster size. This explains the larger discrepancy at small cluster size and its increasing value when more boundary layers are fixed at approximate positions.

These results are interesting since they demonstrate that the use of a cluster geometry with one boundary layer fixed at approximate boundary positions allows to do fast and accurate evaluations of the excess energy of screw dislocations even for small clusters. Similar effects are expected for the DFT calculations since, in metals, the free electron gas screening is very efficient leading to short range surface effects, except in some specific cases where quantum size effects are present [43, 44]. Of course, better evaluations but with heavier calculations can be obtained with exact flexible boundary conditions [26], an approach that should be preferred for very small clusters.

We now apply (2), with 1 FBL at the approximate isotropic elasticity positions, to the calculation of the excess energy within the DFT scheme and for cluster sizes ranging from $N_c = 2 \times 26$ to 2×126 with the IP1 initial position of the dislocation line and $p = 2$ in (4). With this IP, in all calculations the relaxed core is the same asymmetric core (see section 4). As one can see (red circles in figure 3), we do obtain a very good agreement with the theoretical expression of the elastic energy (red curve, equation (1)). The difference between the blue and red curves corresponds mainly to the core energy difference between the EAM and the DFT calculations, since the energy difference between the symmetric and asymmetric DFT cores is of the order of 10 meV/Å (see section 4). Note that the dispersion of the points around the theoretical curve is less than ≈ 8 meV/Å as in the EAM calculation.

It is therefore possible to extract accurate excess energy values with a straightforward and fast calculation of the *total* energy of the cluster with and without the dislocation using the same approximate fixed boundary conditions in both calculations (1 FBL). The value of the core energy E_{core} depends on the chosen core radius r_0 which cannot be defined unambiguously. However, for a given r_0, it is possible to compare the E_{core} obtained for different core configurations (section 4) or with different calculations, EAM and DFT: $E_{\mathrm{core}}(\mathrm{EAM}) \approx 120$ meV/Å for the symmetric core while $E_{\mathrm{core}}(\mathrm{DFT}) \approx 11$ meV/Å for the asymmetric core, with $r_0 = b$ (figure 3). This means that the EAM excess energy is roughly 100 meV/Å higher than the DFT one, since the energy difference between the symmetric and asymmetric core is of the order of 10 meV/Å (see section 4). This overestimation of the prismatic core energy with the ZM EAM potential agrees with its overestimation of the prismatic stacking fault energy compared to DFT [25].

The approach we have just developed for the calculation of the excess dislocation energy in the cluster geometry can also be applied to the determination of the core structure: the displacement field due to the dislocation in the cluster, $\vec{u}_{\mathrm{disloc}}(\vec{r})$ can be partly corrected from the displacement field due to the surface, $\vec{u}_{\mathrm{perfect}}(\vec{r})$ to obtain a more accurate value of the displacement due to the dislocation in an infinite crystal, $\vec{u}(\vec{r})$

$$\vec{u}(\vec{r}) = \vec{u}_{\mathrm{disloc}}(\vec{r}) - \vec{u}_{\mathrm{perfect}}(\vec{r}) \tag{5}$$

where $\vec{u}_{\mathrm{disloc}}(\vec{r})$ and $\vec{u}_{\mathrm{perfect}}(\vec{r})$ are respectively the displacement fields corresponding to the cluster with the dislocation and without it, with the same boundary conditions (1 FBL). This is exactly what we did, and we have not observed any noticeable difference between this displacement field and the exact one deduced from the very large cluster used for the determination of the exact excess energy, except close to the boundary layer and for the smallest considered cluster for which differences are starting to emerge in the core region ($\approx 0.03b = 0.088$ Å for the largest differences). These differences in the core region are small enough to consider that the core structure is rather properly described. From the energetic point of view, their accumulation together with that observed at the boundary region may induce significant errors in the excess energy determination. Nevertheless, as previously mentioned, this is not the case, the errors being less than ≈ 8 meV/Å, i.e. $\approx 3\%$ of the excess energy. Only the use of flexible boundary conditions can allow a reduction of this error in the case of very small clusters.

It should be noted that this approach is certainly limited to the case where the defect displacement field interacts weakly with the cluster surface displacement field, like in the case of screw dislocations. It is doubtful that this method could work with edge dislocations, the main displacement field of which being coplanar with the surface displacement field.

4. Metastable core structure and energies

Having shown that the excess dislocation energy can be extracted with a good accuracy from a DFT cluster calculation at the approximate boundary positions (1 isotropic FBL), it is now possible to investigate the different core structures and compare their corresponding excess energies.

According to the protocol developed in [23], six different IPs (see figure 2) for the origin of the elastic displacement field applied to generate the dislocation before relaxation have been chosen. As in section 3, the systems were prepared such that the atoms were positioned following the linear isotropic elasticity theory with a $\frac{a}{3}[1\,1\,\bar{2}\,0]$ screw dislocation which centre was set at these different IPs. Then the atoms of the cluster boundary layer (1 FBL) were kept fixed and the other atoms were relaxed. The core structures were analysed by computing the dislocation differential displacements (DDs) as defined by Vitek *et al* [13] and using (5). Their edge components are negligible (not presented) and their screw components are reported in figure 4.

From the analysis of the DD maps previously obtained [23] using the ZM potential on clusters of $N_c = 8540$ atoms, we observed that, for three of the IPs, the core relaxed to a basal spreading (IP = 1, 2 and 5) and, for the three other IPs, the spreading is prismatic and symmetric (IP = 3, 4 and 6).

Conversely, our DFT (figure 4) results on clusters of $N_c = 252$ atoms show that all the dislocation cores spread in the prismatic plane. However, the final prismatic core structures can be divided in two groups. Depending on the initial position for the origin of the elastic solution, two types of spreading are found: a symmetric (in reference to the mirror plane [0001]) for the three IPs 3, 4 and 6 and an asymmetric core for the three IPs 1, 2 and 5 (see figure 4). In figure 4, each circle corresponds to a row of atoms along the dislocation direction and an arrow between two rows represents the scaled relative displacement between the rows compared with the perfect crystal as deduced from (5). It should be noticed that the symmetric prismatic spreadings in both the DFT and the EAM calculations are associated to the same IP's (3, 4 and 6) located between two atomic rows in the basal plane, whereas the asymmetric prismatic DFT cores are those leading to a basal spreading in the EAM calculations and are located in between two adjacent basal planes. In the EAM calculations, these last IP configurations are favourable to the development of a basal spreading since the basal stacking fault is low. In the DFT calculations, the higher basal stacking fault prevents the development of a basal spreading and leads to the asymmetric prismatic spreading which can be view as a frustrated basal spreading. In each group, the DD-maps are very similar, only small deviations are visible on the displacement maps. In order to evidence a possible dissociation of the dislocations into partials, we report on figure 5 the partial differential maps corresponding to half the Burger's vector partial dislocations. The (a)symmetric character of the spreading can be more easily observed on figure 5 where the two closed triangles identifying the partials are aligned in a prismatic plane for the symmetric spreading and are in two adjacent prismatic planes for the asymmetric ones. The corresponding dissociation lengths are of the order of 7 Å, a value compatible with the one deduced from the prismatic easy stacking fault and the elasticity theory [25] and comparable to those obtained by Ghazisaeidi and Trinkle [21] in their DFT calculation.

The DFT computed dislocation excess energies (2) of the studied structures with the six different IPs are reported in table 1. The excess energies are very close for the six IPs ($\lesssim 12$ meV/Å difference) and are not classified according to the (a)symmetric character of the dislocation. The excess energy of the three symmetric spreadings are higher than those of the asymmetric for IPs 1 and 5 and lower for IP2. Note that the estimated energy accuracy of our DFT calculations is of 0.1 meV/atom, i.e. 8.4 meV/Å (1.8% of the excess energy) for a
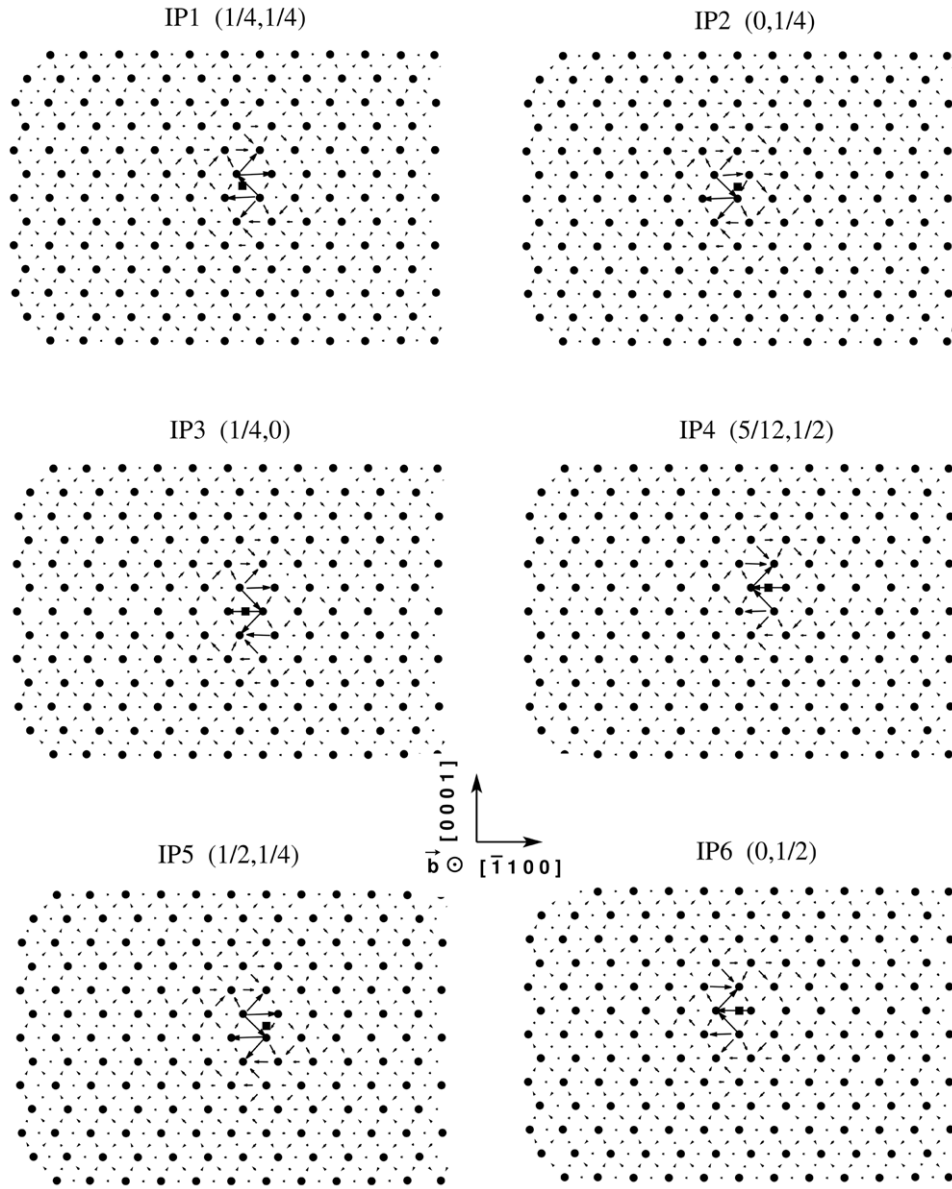
IP1 (1/4,1/4)　　　　　　　　　　　　　　　IP2 (0,1/4)

IP3 (1/4,0)　　　　　　　　　　　　　　　IP4 (5/12,1/2)

$[0001]$

$\vec{b} \odot [\bar{1}100]$

IP5 (1/2,1/4)　　　　　　　　　　　　　　　IP6 (0,1/2)

Figure 4. Hcp Ti $\frac{a}{3}[1\,1\,\bar{2}\,0]$ screw dislocation full DD maps (screw component) for the six IPs of figure 2 calculated within the DFT scheme.

252-atom cluster. The energy differences between the different structures are therefore of the order of the DFT calculation error and of the accuracy of our formulation of the excess energy for small clusters which implies an impossibility to energetically discriminate them.

Nevertheless, we have checked to what extend the structure and the energy of these two different core structures could be affected by the fixed boundary conditions. We have re-optimized (i) the cluster with IP5 (the more stable) with the atoms of the FBL fixed either at the same positions than for IP2 or at the position given by the anisotropic elasticity theory (ii) the cluster with IP2 with the atoms of the FBL fixed at the same positions than for IP5.
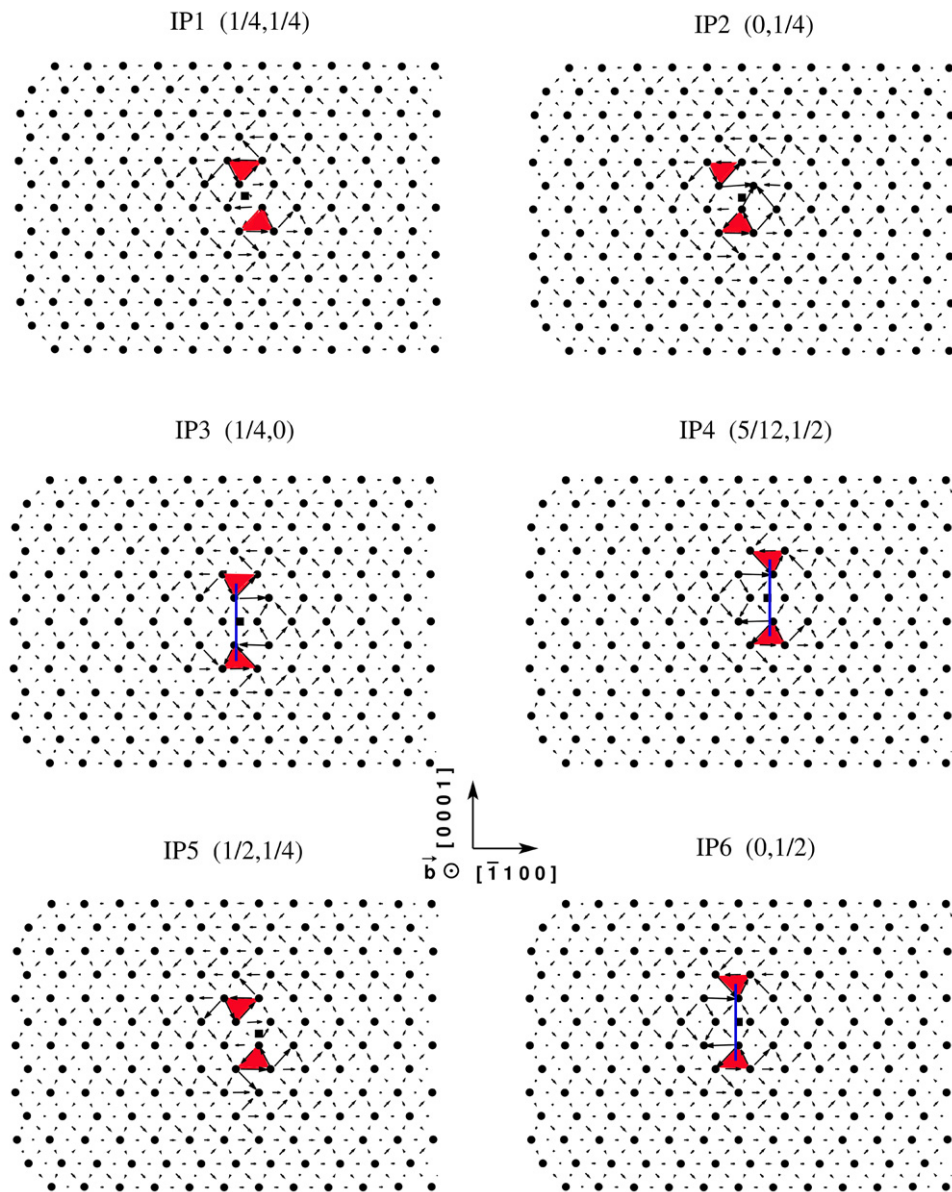
Figure 5. Hcp Ti $\frac{a}{3}[1\,1\,\bar{2}\,0]$ screw dislocation partial DD maps (screw component) for the six IPs of figure 2 calculated within the DFT scheme. The red triangles indicate the positions of the partial dislocations. The blue straight lines indicate the prismatic easy stacking fault.

As a result a modification of the excess energy lower than 2.6% and a modification of the atomic positions lower than 0.7% of the Burgers vector are observed. In agreement with our discussion in section 3, the energy modifications are of the order of the calculation error (1.8%) and do not allow to conclude. However, no important modifications of the core structure are observed which indicates that the obtained (meta)stable cores are stable with respect to the fixed boundary conditions effects. We can therefore be confident in the fact that these two different

Table 1. E_{exc} [eV/Å], the excess dislocation energy deduced from (2) of a $\frac{a}{3}\langle 1\,1\,\bar{2}\,0\rangle$ screw dislocation in hcp-Ti, for the different studied IPs using DFT calculations and the 252-atom cluster with one boundary layer fixed to the isotropic elasticity positions. Bold characters: the symmetric and asymmetric configurations of lowest excess energy.

IP	Core	E_{exc}
1	Asymmetric	0.4396
2	Asymmetric	0.4484
3	Symmetric	**0.4419**
4	Symmetric	0.4425
5	Asymmetric	**0.4364**
6	Symmetric	0.4441
2 with d5 FBL	Asymmetric	0.4525
5 with d2 FBL	Asymmetric	0.4420
5 with anisotropic FBL	Asymmetric	0.4252

core structures do exist, have very close excess energies but, from the present calculation, we cannot infer which one is the most stable one.

Despite our use of fixed boundary conditions instead of flexible ones [26], two core structures have been obtained that are similar to the ones described in our preliminary DFT study [23] with a smaller cluster (2×77 atoms) and the same boundary conditions. These two structures have been next also obtained by Ghazisaeidi and Trinkle [21] in their DFT and MEAM study with flexible boundary conditions. More recently, Rao *et al* [24] have performed a systematic search of metastable structures using the same MEAM potential in a cluster approach with fixed boundary positions, given by the anisotropic elasticity theory, using very large simulation cells. Besides the symmetric and the asymmetric structures, they have obtained three other asymmetric core structures very similar to the previous one and a basal dissociated core similar to the one we have obtained using the EAM potential. Note that the symmetric prismatic dislocation structure is also very similar to the ones obtained on smaller clusters in other previously published electronic structure calculations in the DFT scheme [19, 45], in the tight binding (TB) approach [5, 14] and also in bond order potential calculations [15]. In the MEAM calculations [21, 24], the symmetric core is always the most stable one, by respectively 4 and 1.3 to 4 meV/Å. This very small energy difference is consistent with our DFT estimations of the excess energies of both cores and underlines that their MEAM interaction model is certainly at present the best one to perform dynamical studies as already mentioned in our previous study of the γ-surfaces [25]. However, in our DFT calculation (bold values in table 1) the assymmetric core seems to be more stable than the symmetric. Nevertheless, as previously discussed, the accuracy of our calculations does not allow to conclude definitely.

This DFT study confirms that the fundamental core structure of the $\frac{a}{3}\langle 1\,1\,\bar{2}\,0\rangle$ screw dislocation in Ti is prismatic. Concerning the existence and the configuration of metastable core structures, the situation is more intricate. In all the calculations [5, 14, 18, 19, 46–48] anterior to our preliminary study [23], apart from the prismatic structure, the basal core structure (not observed in the DFT calculations) is the most usually observed one. In his TB calculations, Legrand [5, 14] found other metastable structures: various prismatic cores with different spreading and a core structure intermediate between the prismatic and the basal one which is more stable than the basal one. This last structure can also be seen as intermediate between the basal and the prismatic core structures. Due to the small size of the clusters in the DFT calculations and the approximations involved in the exchange and correlation functional, one cannot definitely exclude the possibility that a basal metastable core exists. However,

it is worth noting that the basal core could not be stabilized in the DFT calculations even when the initial configuration was a pre-dissociated basal core (see also [23])[6]. Consequently, even if it never appears that a basal core is stable, it will be metastable against the symmetric and asymmetric prismatic cores. The basal core obtained by Rao *et al* [24] with the MEAM potential cannot be considered as a definite proof that a basal core is possible. Indeed, as discussed in [25] and contrary to the DFT calculations, the basal stacking fault has a lower excess energy than the prismatic one with the EAM and MEAM potentials which favours the stabilization of a basally dissociated core. With the EAM potential, the basal stacking fault excess energy is so low compared to the prismatic one that the basally dissociated core has a lower excess energy than the prismatic one. With the MEAM potential the difference is smaller, leading to a basal core whose excess energy is slightly higher than the prismatic one. It must be reminded that both the EAM and MEAM potentials are indeed unable to reproduce the flattening of the γ-prismatic surface around the F_1 point, and the local minimum at F_1 which they found to be a saddle point [21, 25]. All these results seem to indicate that the potential energy surface is very flat and that there could be many metastable core structures in hcp-Ti. This is certainly due to the lower symmetry of the hcp lattice compared to cubic lattices and the subsequent anisotropic character of its properties. This could be in favour of the dislocation motion model proposed by Farenc and coworkers [6] to explain the jerky movement of the dislocations, since it relies on the existence of metastable dislocation cores that are more glissile than the stable core. More precisely, since the prismatic plane is the glide plane, the validity of the proposed locking-unlocking mechanism [6] supposes that the sessile dislocation core is the assymmetric core and the glissile one is the symmetric core with a significant energy barrier in between. The calculation of the Peierls stress associated to these core configurations and of the energy barrier between the two cores is therefore necessary to conclude. Ghazisaeidi and Trinkle [21] have shown that, with the MEAM potential, the assymmetric core always reconstructs in the symmetric one in an irreversible way. Rao *et al* [24], with the MEAM potential too, have determined the Peierls stress for the motion of the symmetric core and the kink pair formation energy. They found a very low kink pair formation energy compared to the Peierls stress and thus concluded that the dislocation glide mechanism in the prismatic plane was a kink pair formation mechanism. Their values are compatible with the experimentally observed strain rate [49]. If these results can explain the easy prismatic plane glide in α-Ti, they cannot explain the observed jerky dynamics [6], since the assymmetric core always reconstructs, in an irreversible way, into the symmetric core. As previously discussed, the present uncertainty in the energetic hierarchy between the symetric and the assymetric core leaves still open the possibility of the locking-unlocking mechanism between a sessile stable assymetric core and a glissile symetric core.

5. Electronic structure

In this section, the electronic structure of the 252-atom cluster described above is analysed using DFT, for the asymmetric and symmetric core structures.

The comparison of the *d* partial electronic densities of states (figure 6(*a*)) of a cluster of 252 atoms with and without a prismatic dislocation (IP5) reveals an important redistribution of the occupied states induced by the dislocation. The number of occupied states of high energy (just below the Fermi level) increases and correlatively the number of states of low energy

---

[6] In [23] we found a stable basal dislocation core when the initial configuration was the basal core obtained with the IP2 in the EAM calculation. However this result was obtained with a smaller cluster (2×77) and with less stringent convergence criteria than in the present study (2×126) where this basal core reconstructs into the asymmetric core.
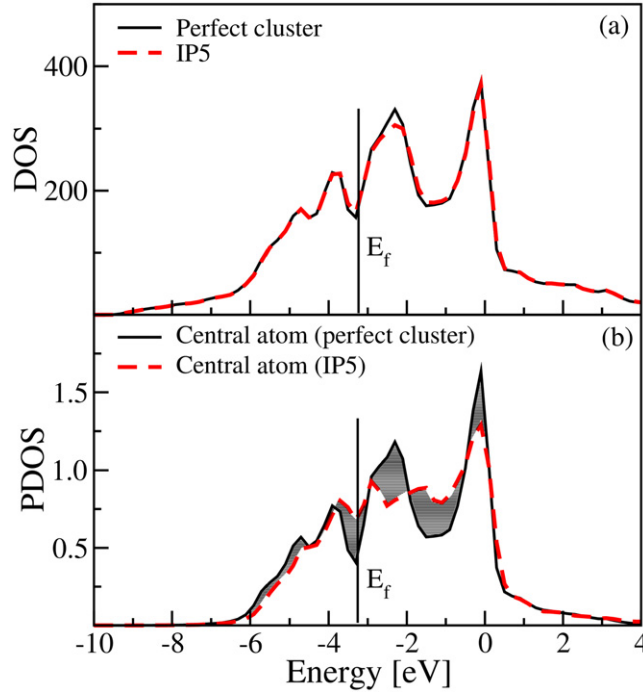
Figure 6. Partial *d* electronic density of states (PDOS) for a cluster of 252 atoms with (red dashed line) and without (black line) the IP5 asymmetric dislocation core. (*a*): the whole cluster, (*b*): the central atom. The dashed surface corresponds to the difference between the two PDOS.

decreases (not visible at the scale used in the figure). Consequently, there is an increase of the Kohn–Sham electronic energy which contributes to the excess dislocation energy. One can also note a decrease of the peak just above the Fermi level. Since most of the atoms of the cluster are only slightly perturbed by the presence of the dislocation, the observed differences seem rather small. However, these differences mainly come from the *d* states of the 'core' atoms. This is visible in figure 6(*b*), where the *d*-PDOS on the central atom of the 252-atom cluster with and without the dislocation are presented. The *d* states of the atoms localized at the centre of the cluster are modified by the introduction of the screw dislocation. Similarly all the atoms close to the dislocation IP present a modified *d*-PDOS compared to that of the central atom in the perfect lattice.

These large local changes of the electronic structure around the Fermi level visible in the *d*-PDOS can be used as an alternative way of potentially defining the 'core' region from an electronic point of view. Figure 7 shows these variations as the normalized difference between the atom *d*-PDOS with and without the dislocation, for a 252-atom cluster. In this figure, a colored circle with identical arbitrary diameter (4.6 Å) is drawn around each atom using a different color, depending on the following calculated quantity:

$$\Delta\text{PDOS}(j) = \frac{\sum_i |\text{PDOS}^{\text{dis}}(i, j) - \text{PDOS}^{\text{perfect}}(i, j)|}{\sum_i \text{PDOS}^{\text{perfect}}(i, j)}, \tag{6}$$

where $\text{PDOS}^{\text{dis}}(i, j)$ and $\text{PDOS}^{\text{perfect}}(i, j)$ are, respectively, the *d*-PDOS of atom *j* for the energy e_i, the summation over *i* extending over the whole *d* band. With this definition,
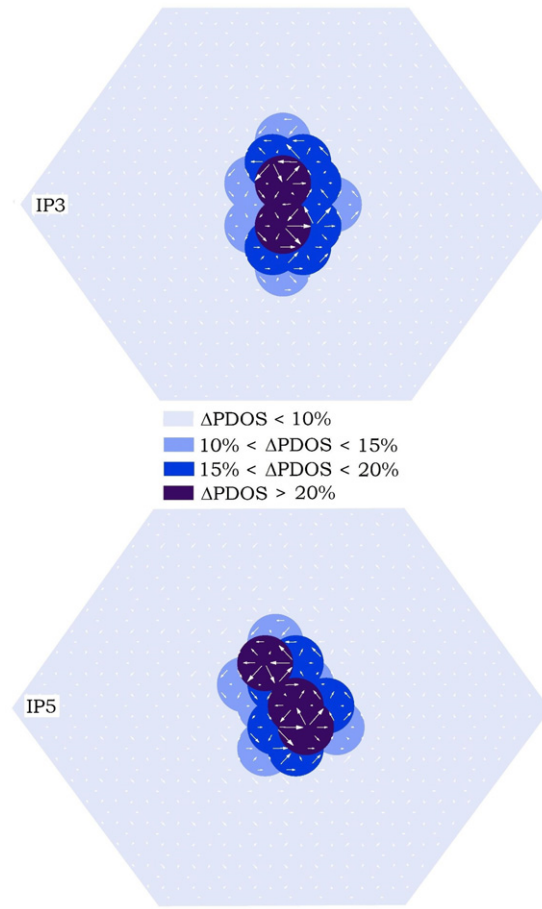
Figure 7. Variation of the population of the d states induced by the introduction of the screw dislocation in a 252-atom cluster. Up: IP3 symmetric core. Down: IP5 asymmetric core.

ΔPDOS(j) is a measure of the dashed area shown in figure 6, for each atom. The results presented in figure 7 show that the atoms with the largest ΔPDOS are localized in an elongated cylinder along the [0 0 0 1] direction with a radius of 10 Å in the [0 0 0 1] direction and 5 Å in the [$\bar{1}$ 1 0 0] direction, what is quite similar to the geometry observed in the DD maps. It should be noticed that the d-PDOS modification is symmetric in reference to the mirror plane [0 0 0 1] for the symmetric spreading (IP3) and asymmetric for the non-symmetric spreading (IP5). The study of the d-state modification induced by the introduction of the screw dislocation seems to allow not only the evaluation of the core extension (ΔPDOS(j) > 10%) but also the determination of the (a)symmetric character of the defect.

6. Conclusion

A straightforward and fast ansatz, applicable in a DFT calculation, has been proposed for the calculation of the excess energy, per unit length of dislocation, of an infinite straight

screw dislocation in an infinite crystal, using approximate boundary conditions in a cluster calculation. More precisely, we proposed an expression of $E_{\text{exc}}(r)$, the excess dislocation energy stored in a cylinder of radius r centred on the dislocation line. It is applicable in a DFT calculation because it relies on the calculation of the total energy of clusters, hexagonal shaped cylinders centred on the dislocation line whose hexagonal section is the same as that of the corresponding disc of radius r. The ansatz for $E_{\text{exc}}(r)$ is simply given by the difference between the total energies of the cluster with and without the dislocation, calculated with the same approximate boundary condition. The method has been validated with a semi-empirical EAM interaction model for which exact calculations of $E_{\text{exc}}(r)$ can be performed. In order to obtain an accurate value of $E_{\text{exc}}(r)$ both calculations must be performed with only one FBL at the perfect crystalline positions for the cluster without the dislocation and at approximate boundary conditions with the dislocation, as those given by the elastic theory isotropic or anisotropic for example. The method is quite accurate since the error is negligible for large clusters and that, even if it increases with decreasing values of r, it remains of the order of 1.5% of the excess energy for the smallest considered cluster ($r = 9.95$ Å, 26 atoms per plane normal to the dislocation line). The method has then been applied to the DFT study of one core structure of the $\frac{a}{3}\langle 1\,1\,\bar{2}\,0\rangle$ screw dislocation in Ti with different cluster sizes. The expected $\ln r$ dependence of the excess energy has been recovered with the same accuracy as in the EAM calculation, an extra proof of the validity of the method.

This method opens then the possibility to study the relative energetic stability of different core structures in the very accurate DFT scheme, as presented here for the $\frac{a}{3}\langle 1\,1\,\bar{2}\,0\rangle$ screw dislocation in Ti. An extensive search of its (meta)stable configurations has been performed through accurate DFT calculations of $E_{\text{exc}}(r)$, for different initial conditions. We have evidenced the existence of two different core structures: a symmetric and an asymmetric one. An alternative way of defining the core region from an electronic structure point of view has been proposed and used to characterize these two dislocation cores. The excess energy difference between these two prismatic cores is within the uncertainty of our calculations and, thus, we cannot conclude concerning their energetic ordering. Our results combined with previous studies [5, 14, 15, 19, 21, 23, 45] seem to indicate that there exist many metastable core structures in hcp-Ti. Moreover, from our excess energy calculations, they are probably located in a very narrow energy range. Such small energy differences will not be easy to reproduce with empirical models and can be used for the validation of such interaction models for the dynamical study of the $\frac{a}{3}\langle 1\,1\,\bar{2}\,0\rangle$ screw dislocation in Ti.

We are presently working on a theoretical justification of the validity of our ansatz, an improved and more accurate formulation based on the use of exact boundary conditions, and applicable to the general calculation of excess energies of defects in the cluster approach.

References

[1] Hirth J P and Lothe J 1982 *Theory of Dislocations* 2nd edn (Malabar, FL: Krieger Publishing Company)
[2] Caillard D and Martin J-L 2003 *Thermally Activated Mechanisms in Crystal Plasticity* (Oxford: Pergamon)
[3] Yoo M H, Morris J R, Ho K M and Agnew S R 2002 Nonbasal deformation modes of hcp metals and alloys: role of dislocation source and mobility *Metall. Mater. Trans.* A **33** (3, special issue) 813–22 *Annual Meeting of the TMS (New Orleans, LA, 11-15 February 2001)*
[4] Bacon D and Vitek V 2002 Atomic-scale modeling of dislocations and related properties in the hexagonal-close-packed metals *Metall. Mater. Trans.* A **33** 721–33

[5] Legrand B 1984 Influence de la structure électronique sur la facilité relative des glissements dans les métaux de structure hexagonale compacte *PhD Thesis* Université Pierre et Marie Curie, Paris, France

[6] Farenc S, Caillard D and Couret A 1993 An *in situ* study of prismatic glide in α titanium at low temperatures *Acta Metall. Mater.* **41** 2701–9

[7] Caillard D 2009 Tem '*in situ*' straining experiments in fe at low temperature *Phil. Mag. Lett.* **89** 517–26

[8] Caillard D 2010 Kinetics of dislocations in pure Fe: Part II. *In situ* straining experiments at low temperature *Acta Mater.* **58** 3504–15

[9] Lu G, Kioussis N, Bulatov V V and Kaxiras E 2000 Generalized-stacking-fault energy surface and dislocation properties of aluminum *Phys. Rev.* B **62** 3099–108

[10] Ismail-Beigi S and Arias T A 2000 *Ab initio* study of screw dislocations in Mo and Ta: a new picture of plasticity in bcc transition metals *Phys. Rev. Lett.* **84** 1499–502

[11] Woodward C and Rao S I 2002 Flexible *ab initio* boundary conditions: simulating isolated dislocations in bcc Mo and Ta *Phys. Rev. Lett.* **88** 216402

[12] Woodward C, Trinkle D R, Hector L G Jr and Olmsted D L 2008 Prediction of dislocation cores in aluminum from density functional theory *Phys. Rev. Lett.* **100** 045507

[13] Vitek V, Perrin R C and Bowen D K 1970 The core structure of $1/2\langle 1\,1\,1\rangle$ screw dislocations in bcc crystals *Phil. Mag.* **21** 1049–73

[14] Legrand B 1985 Structure du coeur des dislocations vis $1/3a\langle 1\,1\,\overline{2}\,0\rangle$ dans le titane *Phil. Mag.* A **52** 83–97

[15] Girshick A, Pettifor D G and Vitek V 1998 Atomistic simulation of titanium: II. Structure of $1/3\langle \overline{1}\,2\,\overline{1}\,0\rangle$ screw dislocations and slip systems in titanium *Phil. Mag.* A **77** 999–1012

[16] Morris J R, Ho K M, Chen K Y, Rengarajan G and Yoo M H 2000 Large-scale atomistic study of core structures and energetics of $\langle c + a\rangle 1\,1\,\overline{2}\,2$ dislocations in hexagonal close packed metals *Model. Simul. Mater. Sci. Eng.* **8** 25

[17] Pasianot R, Zie Z, Farkas D and Savino E J 1994 Computer simulation of $\langle 1\,0\,0\rangle$ dislocation core structure in NiAl *Model. Simul. Mater. Sci. Eng.* **2** 383

[18] Domain C 2002 Simulations atomiques ab-initio des effets de l'hydrogène et de l'iode dans le zirconium *PhD Thesis* Université des Sciences et Technologies de Lille

[19] Domain C and Legris A 2004 Investigation of glide properties in hexagonal titanium and zirconium: an *ab initio* atomic scale study *Iutam Symp. on Mesoscopic Dynamics of Fracture Process and Materials Strength* **115** 411–20

[20] Cai W, Bulatob V V, Chang J, Li J and Yip S 2003 Periodic image effects in dislocation modelling *Phil. Mag.* **83** 539–67

[21] Ghazisaeidi M and Trinkle D R 2012 Core structure of a screw dislocation in ti from density functional theory and classical potentials *Acta Mater.* **60** 1287–92

[22] Clouet E 2012 Screw dislocation in zirconium: an *ab initio* study *Phys. Rev.* B **86** 144104

[23] Tarrat N, Benoit M and Morillo J 2009 Core structure of screw dislocations in hcp Ti: an *ab initio* DFT study *Int. J. Mater. Res.* **3** 329–32

[24] Rao S I, Venkateswaran A and Letherwood M D 2013 Molecular statics and molecular dynamics simulations of the critical stress for motion of a/3 screw dislocations in α-Ti at low temperatures using a modified embedded atom method potential *Acta Mater.* **61** 1904–12

[25] Benoit M, Tarrat N and Morillo J 2013 Density functional theory investigation of the titanium γ-surfaces and stacking faults *Modelling Simul. Mater.* **21** 015009

[26] Rao S, Hernandez C, Simmons J P, Parthasarathy T A and Woodward C 1998 Green's function boundary conditions in two-dimensional and three-dimensional atomistic simulations of dislocations *Phil. Mag.* A **77** 231–56

[27] Soler J M, Artacho E, Gale J D, García A, Junquera J, Ordejón P and Sánchez-Portal D 2002 The siesta method for *ab initio* order-N materials simulation *J. Phys.: Condens. Matter* **14** 2745–79

[28] Perdew J P, Burke K and Ernzerhof M 1996 Generalized gradient approximation made simple *Phys. Rev. Lett.* **77** 3865–8

[29] Troullier N and Martins J L 1991 Efficient pseudopotentials for plane-wave calculations *Phys. Rev.* B **43** 1993–2006

[30] Daw M S and Baskes M I 1983 Semiempirical, quantum mechanical calculation of hydrogen embrittlement in metals *Phys. Rev. Lett.* **50** 1285–8

[31] Zope R R and Mishin Y 2003 Interatomic potentials for atomistic simulations of the Ti–Al system *Phys. Rev.* B **68** 024102

[32] Hammerschmidt T, Kersch A and Vogl P 2005 Embedded atom simulations of titanium systems with grain boundaries *Phys. Rev.* B **71** 205409

[33] Martin R M 2008 *Electronic Structure : Basic Theory and Practical Methods* (Cambridge: Cambridge University Press)

[34] Chetty N and Martin R M 1992 First-principles energy density and its applications to selected polar surfaces *Phys. Rev.* B **45** 6074–88

[35] Rapcewicz K, Chen B, Yakobson B and Bernholc J 1998 Consistent methodology for calculating surface and interface energies *Phys. Rev.* B **57** 7281–91

[36] Ramprasad R 2002 First-principles energy and stress fields in defected materials *J. Phys.: Condens. Matter* **14** 5497

[37] Rodriguez J I, Ayers P W, Gotz A W and Castillo-Alvarado F L 2009 Virial theorem in the Kohn–Sham density-functional theory formalism: accurate calculation of the atomic quantum theory of atoms in molecules energies *J. Chem. Phys.* **131** 021101

[38] Yu M, Trinkle D R and Martin R M 2011 Energy density in density functional theory: application to crystalline defects and surfaces *Phys. Rev.* B **83** 115113

[39] Bader R F W 1994 *Atoms in Molecules: A Quantum Theory* (Oxford: Clarendon Press)

[40] Christian J W and Vitek V 1970 Dislocations and stacking faults *Rep. Progress Phys.* **33** 307

[41] Schoeck G 1997 The peierls dislocation: line energy, line tension, dissociation and deviation *Acta Mater.* **45** 2597–605

[42] Chrzan D C, Sherburne M P, Hanlumyuang Y, Li T and Morris J W 2010 Spreading of dislocation cores in elastically anisotropic body-centered-cubic materials: the case of gum metal *Phys. Rev.* B **82** 184202

[43] Feibelman P J 1983 Static quantum-size effects in thin crystalline, simple-metal films *Phys. Rev.* B **27** 1991–6

[44] Boettger J C 1996 Persistent quantum-size effect in aluminum films up to twelve atoms thick *Phys. Rev.* B **53** 13133–7

[45] Domain C and Legris A 2005 Ab initio atomic-scale determination of point-defect structure in hcp zirconium *Phil. Mag.* **85** 569–75

[46] Basinski Z S, Duesbery M S and Taylor R 1970 Screw dislocation in a model sodium lattice *Phil. Mag.* **21** 1201–21

[47] Bacon D J and Martin J W 1981 The atomic structure of dislocations in hcp metals: I. Potentials and unstressed crystals *Phil. Mag.* A **43** 883–900

[48] Girshick A, Bratkovsky A M, Pettifor D G and Vitek V 1998 Atomistic simulation of titanium: I. A bond-order potential *Phil. Mag.* A **77** 981–97

[49] Biget M P and Saada G 1989 Low-temperature plasticity of high-purity α-titanium single crystals *Phil. Mag.* A **59** 747–57